# Small and Compact Double E-shaped Meander Line Monopole Antenna for Forward Scatter Radar Network

N. Ripin, M. S. M. Zaman, A. A. Sulaiman, N. E. A. Rashid, M. F. Hussin, W. Z. W. Ibrahim, N. N. Ismail
*Faculty of Electrical Engineering, Universiti Teknologi MARA, Shah Alam, Malaysia.*
*nabilahripin@yahoo.com*

***Abstract*—A small and compact printed monopole antenna can be obtained by introducing double E-shaped meander line patch backed by a partial ground plane. The double E-shaped meander line patch reduces the antenna resonant frequency so that the size of the antenna can be reduced for targeted frequency of 400 MHz specific for Forward Scatter Radar (FSR) Network. 77% size reduction of the antenna has been successfully achieved where the overall size of the proposed antenna is only 93.8 x 131 mm$^2$ (0.125$\lambda_0$ x 0.175$\lambda_0$) compared to before it was reduced which is 190.7 x 276.3 mm$^2$ (0.25$\lambda_0$ x 0.368$\lambda_0$). The size reduction is obtained without significant effects on other antenna performances. The proposed antenna produces high measured efficiency of 85.5% and measured gain of 0.3 dBi with an omnidirectional radiation pattern. A comprehensive parametric study is accomplished to obtain the best performances of the antenna. For a better understanding on the design characteristics, an equivalent circuit model is derived carefully.**

***Index Terms*—Double E-shaped Patch; Equivalent Circuit Model; FSR; Meander Line; Printed Monopole Antenna.**

## I. INTRODUCTION

Forward Scatter Radar (FSR) is a type of bistatic radar that applied for target detection and classification that corresponds to the case when the bistatic angle nearly 180$^0$ [1]. FSR utilizes an effect of electromagnetic wave shadowing a target instead of scattering from the target [2]. Currently, FSR network functions in the Very High Frequency (VHF) and Ultra High Frequency (UHF) channels. The VHF channel is used for target detection and parameter estimation, whereas the UHF channel is used for automatic target recognition.

FSR network consists of several sensor nodes with each sensor has a number of omnidirectional antennas. The sensors are freely dropped from unmanned aerial vehicle to the ground surface [3]. Each sensor consists of omnidirectional antennas in a separate transmitter and receiver [4]. Small antenna size is required to make the sensors smaller, so that the sensors are less complex and cheaper. The power consumption would be lower and the automatic target recognition channel become less power hungry [5].

Antenna miniaturization techniques become antenna designer's interest since a decade ago. Techniques such as metamaterial, slot loaded, inductive and dielectric loading, and fractal technology have been proposed to miniaturized the size of the antenna [6]–[10]. U-shaped and inverted U-shaped metamaterial is loaded in the antenna design to miniaturized the size of the dual-band planar antenna [6]. The proposed method produces reduction in antenna size of 77%.

Das et al proposed a slotted microstrip antenna with modified ground plane. The size of the antenna was reduced up to 67% by applying the proposed method. Kramer et al reported an ultra-wideband (UWB) spiral antenna. The size of the spiral antenna was reduced approximately by 50% using dielectric and inductive loading.

Multiple band-notched characteristic of UWB printed monopole antenna is proposed in [11] using four pairs of meander lines. The meander lines placed along the edge of the microstrip line and ground plane produce quadruple band-notch characteristic without increasing the antenna size.

Small triple-band microstrip antenna for WLAN/WiMAX applications was reported in [12]. The size of the reported antenna is reduced to 19 x 25 mm$^2$ (0.152$\lambda_0$ x 0.2$\lambda_0$) using the combination of slots and DGS.

In this study, a small printed monopole antenna for FSR network is presented. The size of the proposed antenna is miniaturized based on the slots and meander line technique which produces a novel structure of double E-shaped meander line patch. The excellent performances of the proposed antenna was obtained from the comprehensive parametric analysis. From the novel structure topology, an equivalent circuit model has been derived. The idea of modelling the equivalent circuit is taken from several literatures such as in [13]–[19].

## II. METHODOLOGY

The printed monopole antenna basically consists of a square radiating patch of width *Ws* and length *Ls* printed on a substrate of dielectric constant $\varepsilon_r$ and thickness *h*. The antenna has a partial ground plane of length *Lg* on the other side. Figure 1 shows the typical printed monopole antenna which referred to as reference antenna which was designed on the FR-4 substrate with $\varepsilon_r$ = 4.3, and thickness *h* = 1.6 mm. The antenna is constructed based on the ordinary design procedure to define the width (*Wp*) and length (*Lp*) of the radiating patch for covering 400 MHz operating frequency. It is fed by 50 Ω transmission line of width *Wf* and length *Lf*. In this study, all antennas were designed, simulated and optimized using Computer Simulation Technology (CST) software.

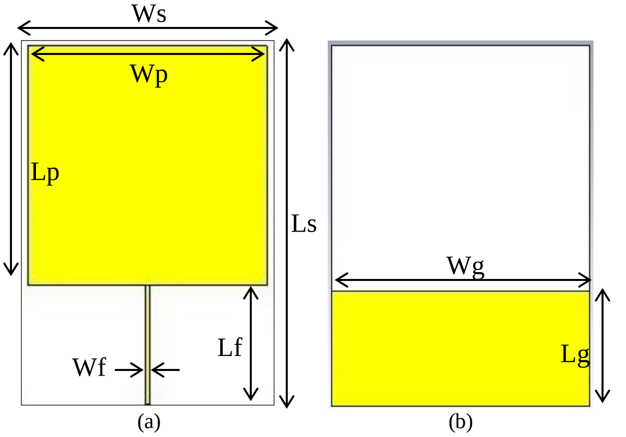


Figure 1: Reference antenna geometry (a) front view (b) back view

Figure 2 shows the development of the antennas from the reference antenna to the double E-shaped meander line monopole antenna. Figure 2 (a) shows the configuration of the reference antenna. Modification was made onto the radiating patch by introducing slots as illustrated in Figure 2 (b) to reduce the antenna resonant frequency. The slots were inserted on the patch where the strongest current path is concentrated in order to increase the effective current distribution. By increasing the current distribution on the radiator, the effective capacitance and inductance will be increased as well, which then decrease the resonant frequency of the antenna. More slots were introduced on the radiator which resulting in double E-shaped patch structure as shown in Figure 2 (c). After that, the thin line on the middle of the patch was replaced by the meander line to further increase the effective inductance and capacitance as demonstrated in Figure 2 (d). All antenna structures in Figure 2 have the same dimensions except for the slots and meander line.

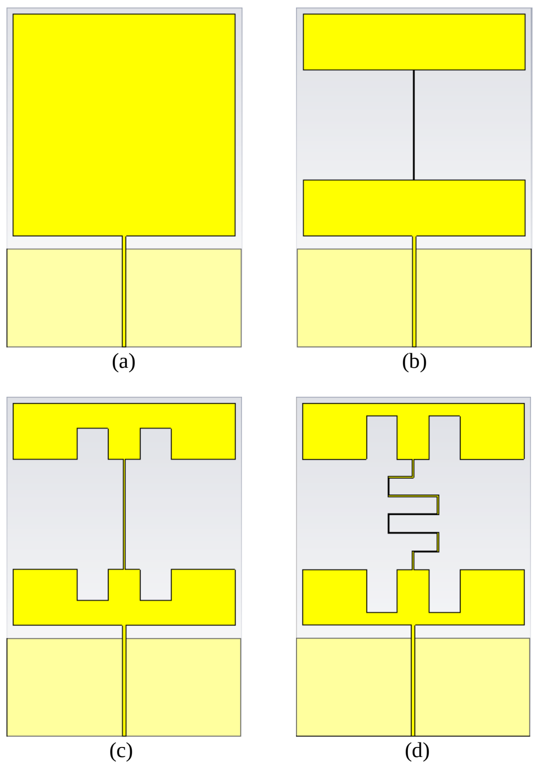


Figure 2: Development of the antenna design

The patch area of the double E-shaped meander line monopole antenna is enlarged for visibility as demonstrated in Figure 3. All the parameters of the antennas are listed in Table 1 with the values are organized in millimeter (mm).

Table 1
Parameters of Double E-shaped Meander Line Antenna

| Parameters | Value (mm) | Parameters | Value (mm) |
|---|---|---|---|
| Ws | 190.7 | a | 90 |
| Ls | 276.3 | $l_1$ | 35.17 |
| Wp | 181.1 | la | 14.17 |
| Lp | 181.1 | wa | 19.20 |
| Wf | 3.1 | wb | 41.50 |
| Lf | 90.4 | wc | 1.0 |
| Wg | 190.7 | $w_1$ | 35.17 |
| Lg | 80.2 | $w_2$ | 26.0 |

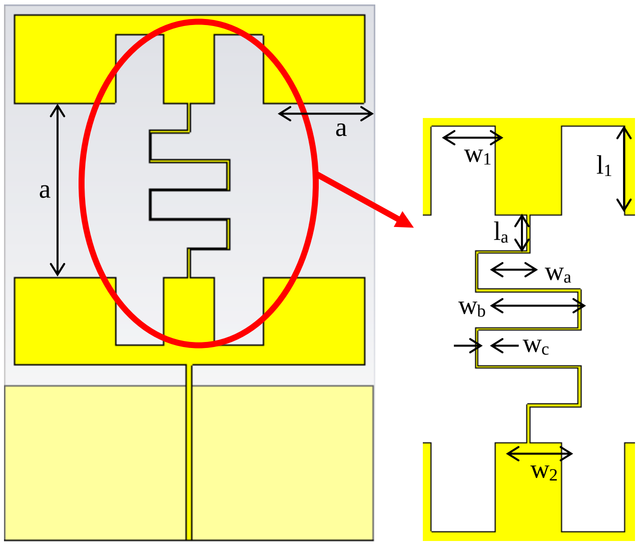


Figure 3: Double e-shaped meander line monopole antenna with meander line area is enlarged for visibility.

## III. PARAMETRIC STUDY

The parametric study is performed to provide the best antenna performances using optimization. The performance of the antenna is mostly affected by electrical antenna parameters including the dimensions of the ground plane, slots and meander line. Figure 4 displays the effects of various length of the ground plane, *Lg* on the simulated reflection coefficient. It is found that the length of the ground plane is optimum at *Lg* = 90 mm.

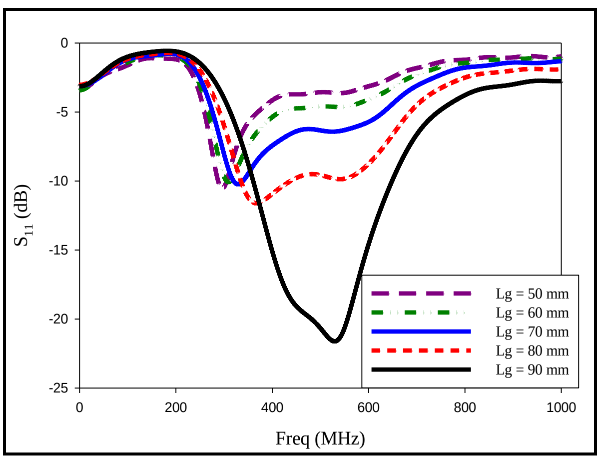


Figure 4: Simulated reflection coefficients for various *Lg*

Figure 5 presents the simulated reflection coefficients for various *a*. It is clearly seen in the graph that the resonant frequency decreased as the width/length of the slot increased. The optimum width/length of the slot is at $a$ = 90 mm where the antenna resonates at 231 MHz.

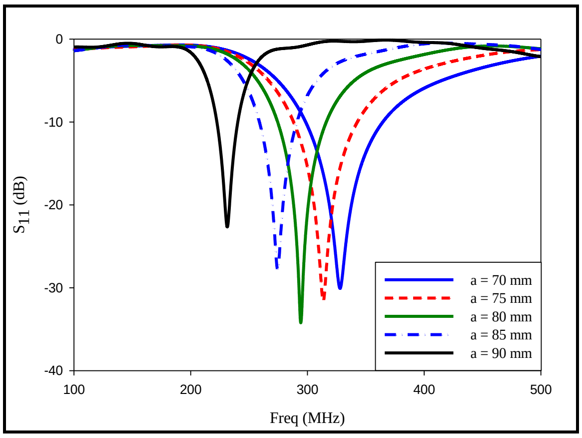


Figure 5: Simulated reflection coefficients for various *a*

The width of the added slot $w_1$ is varied to observe its effects on the simulated reflection coefficient as illustrated in Figure 6. From the graph, the resonant frequency is at the lowest band when $w_1$ = 35.17 mm. Figure 7 portrays the simulated reflection coefficients for various $l_1$. It is found that the length of the slot is optimum at $l_1$ = 35.17 mm.

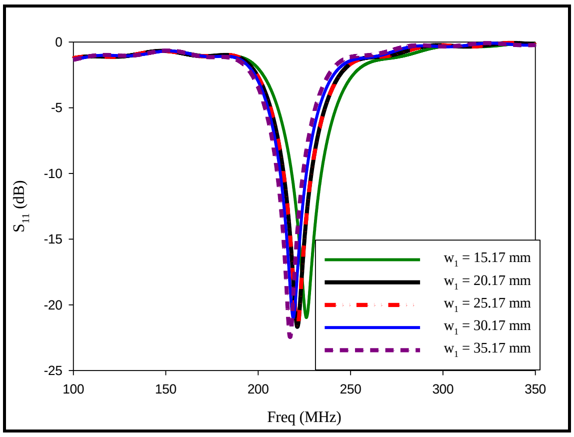


Figure 6: Simulated reflection coefficients for various $w_1$

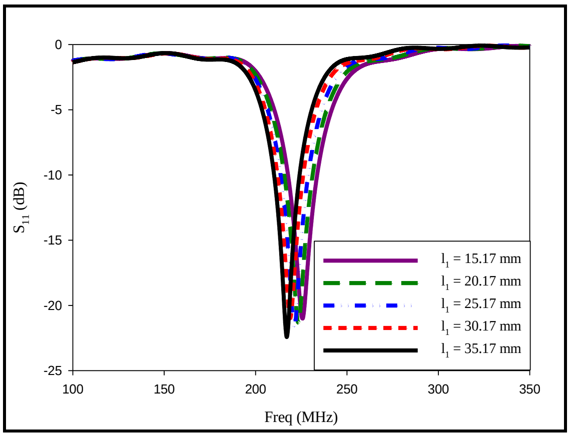


Figure 7: Simulated reflection coefficients for various $l_1$

The dimensional parameter of the meander line on the double E-shaped meander line monopole antenna is varied to observe its effects on the antenna performances as depicts in Figure 8. From the graph, the resonant frequency is decreased to 186 MHz as the $w_a$ increased to 19.2 mm.

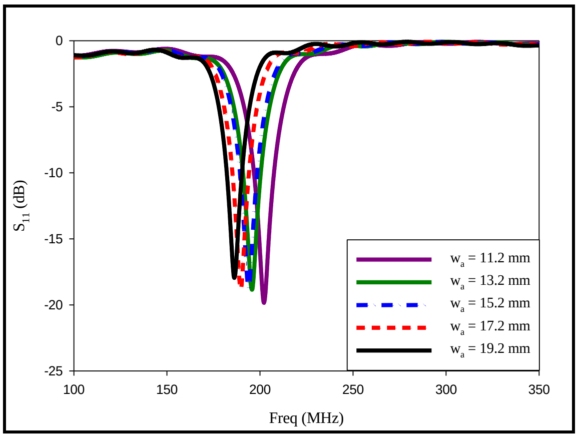


Figure 8: Simulated reflection coefficients for various $w_a$

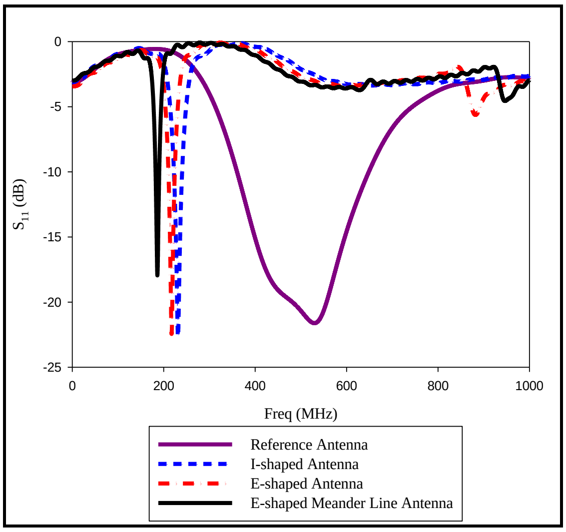


Figure 9: Simulated reflection coefficients for various antenna designs

The performances of the antennas evolution (in Figure 2) are demonstrated clearly in Figure 9. It is observed that, every antenna resonates with different center frequency. The reference antenna possesses broad band characteristics covering 357 MHz to 646 MHz. The resonant frequency is reduced as the slots were introduced on the antenna. I-shaped antenna resonates at 231 MHz with a narrow bandwidth due to the modification on the patch area. The resonant frequency is further reduced as more slots were added onto the patch. The added slots produce the double E-shaped patch structure which resonates at 217 MHz. When meander line was proposed to the design, the antenna resonant frequency shifted to 186 MHz. It is noticed that the modification on the radiator causes reduction in antenna resonant frequency and impedance bandwidth. The narrow band characteristics of the antenna do not affect the target application of Forward Scatter Radar (FSR) Network does not require wide band antenna.

## IV. Result and Discussion

As explained earlier, the resonant frequency of the antenna is shifted to the lower band when the proposed method is applied. The next step is to reduce the antenna size so that the antenna will resonate with targeted frequency of 400 MHz. The overall size of the double E-shaped meander line monopole antenna was reduced by 77% to achieve 400 MHz center frequency. The miniaturized antenna is referred as proposed antenna with its dimensional parameters are listed in Table 2. The area of the proposed antenna is only 93.8 x 131 $mm^2$. The proposed antenna has been fabricated on the FR-4 substrate using LPKF milling machine. Figure 10 displays the photograph of the fabricated proposed antenna. The experimental works have been carried out in Anechoic Chamber using Vector Network Analyzer (VNA) to validate and verify the antenna performances.

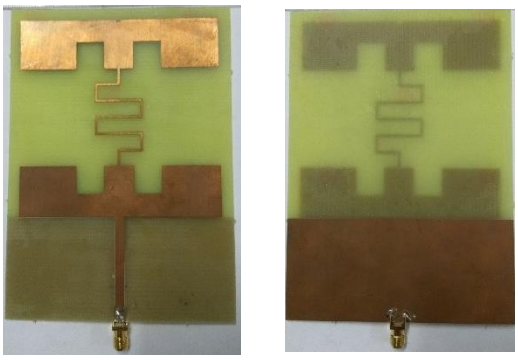

(a) (b)

Figure 10: Photograph of the fabricated antenna (a) front view (b) back view

Table 2
Parameters of Miniaturized Double E-shaped Meander Line Antenna

| Parameters | Value (mm) | Parameters | Value (mm) |
|---|---|---|---|
| Ws | 93.8 | a | 41.6 |
| Ls | 131.0 | $l_1$ | 11.7 |
| Wp | 84.2 | la | 6.1 |
| Lp | 84.2 | wa | 10.6 |
| Wf | 3.6 | wb | 20.2 |
| Lf | 42.0 | wc | 1.0 |
| Wg | 93.8 | $w_1$ | 11.7 |
| Lg | 41.8 | $w_2$ | 12.6 |

The simulated and measured reflection coefficients of the proposed antenna are demonstrated in Figure 11. Both results are agreeing well with each other with their performance are organized in Table 3. Figure 12 shows the simulated and measured 2D radiation pattern of the proposed antenna. From the plot, the proposed antenna produces omnidirectional radiation pattern.

The performances comparison between the simulated and measured proposed antenna is organized in Table 3. The proposed antenna produces acceptable simulated and measured antenna gain of 1.5 dBi and 0.3 dBi, respectively. The discrepancies between the antenna gain might be due to the electrically small antenna size and ground plane. The proposed antenna possesses a very high antenna efficiency of 85.5 %.

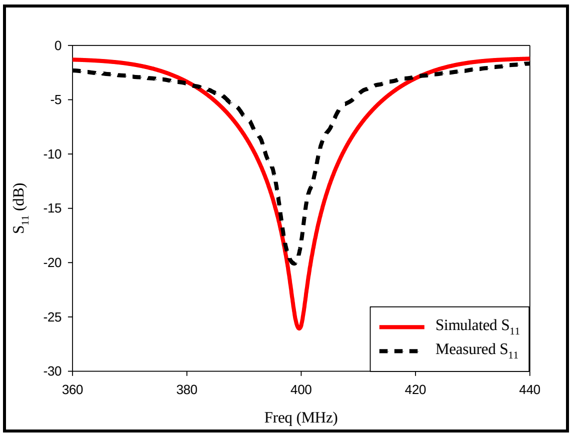


Figure 11: Simulated and measured reflection coefficient of the proposed antenna

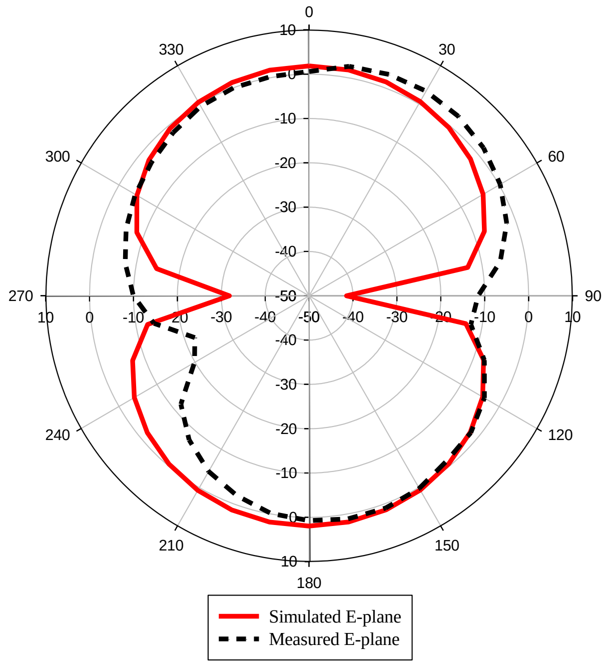


Figure 12 Simulated and measured radiation pattern of the proposed antenna

Table 3
Comparison of Simulated and Measured Performances of Miniaturized Proposed Antenna

| Parameters | Simulation | Measured |
|---|---|---|
| Reflection coefficient, $S_{11}$ (dB) | -25.80 | -20.70 |
| Resonant Frequency (MHz) | 400 | 398.7 |
| Directivity (dB) | 1.97 | 0.58 |
| Gain (dBi) | 1.5 | 0.3 |
| VSWR | 1.1 | 1.2 |
| Bandwidth (MHz) | 15.2 | 9.2 |
| Efficiency (%) | 90.0 | 85.5 |

In this study, the antenna circuit model was developed to provide better understanding of the antenna characteristics and expose the physics behind the structure. The equivalent lumped element circuit is generated based on the antenna input impedance as in Figure 13 where the input impedance of the antenna is considered as a two terminal device comprising an arbitrary set of lumped resistors $R$, capacitors $C$ and inductors $L$ connected either in series or parallel. The equivalent circuit model displayed in Figure 14 represents the proposed antenna which was designed using Advance Design System (ADS) software. The capacitance $C$ and inductance $L$

in the circuit is calculated using equations 1 and 2 [20].

$$l_C = \frac{\lambda_L \omega C Z_l}{2\pi} \quad (1)$$

$$l_L = \frac{\lambda_H \omega L}{2\pi Z_h} \quad (2)$$

where $l_C$ and $l_L$ are the length of the transmission line. While $Z_l$ and $Z_h$ are the lowest and highest realizable characteristics impedances in the medium, respectively. $\lambda_L$ and $\lambda_H$ are the corresponding wavelength related to the free space wavelength $\lambda_0$.

$$\lambda_{L,H} = \frac{\lambda_0}{\sqrt{\varepsilon_{eff}}} \quad (3)$$

Comparison between the simulated result and the circuit model is obtained in Figure 15. It is clearly seen that the performances of the proposed antenna both in EM simulation and circuit simulation agree well with each other.

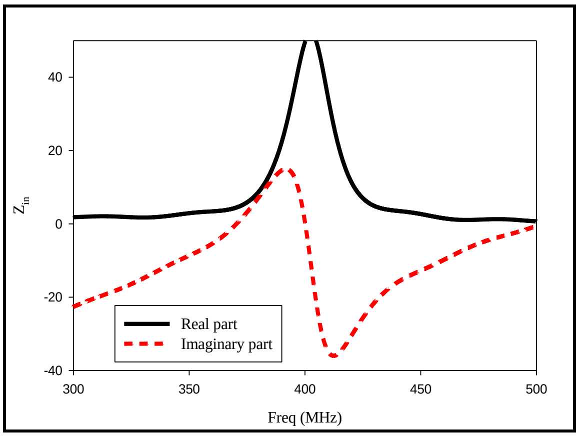


Figure 13: Simulated input impedance of the proposed antenna.

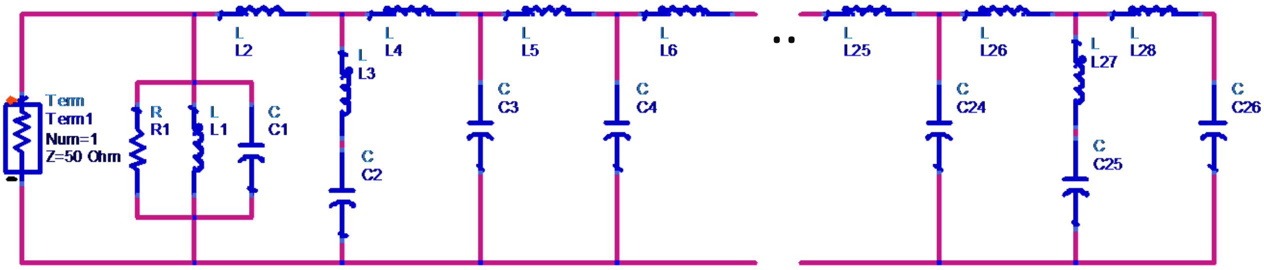


Figure 14: Equivalent circuit model of the proposed antenna

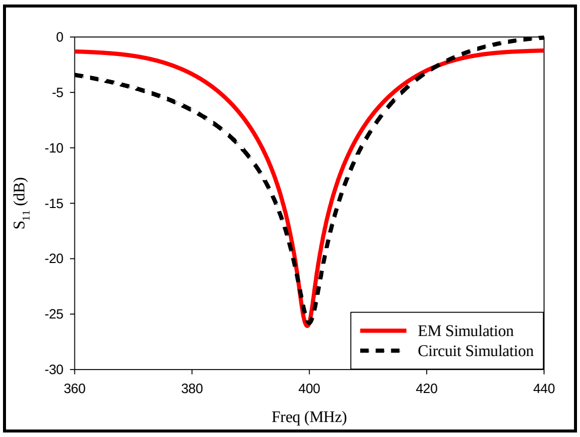


Figure 15: Reflection coefficient of the proposed antenna in EM simulation and circuit simulation

## V. Conclusion

A small and compact double E-shaped meander line printed monopole antenna was designed, optimized, fabricated and tested for FSR applications. The proposed antenna achieves 77% size reduction with a little trade off of other antenna performances. As a matter of fact, the size of the antenna can be decreased more by increasing the dimension of the slots and meander line. However, it would affect the antenna gain and efficiency as well. The antenna gain would be too low if the size of the proposed antenna is decreased more than 77%. The proposed antenna produces omnidirectional radiation pattern of acceptable antenna gain. Parametric studies were carried out to offer good antenna performances while the equivalent circuit model was derived to provide better understanding on the physics behind the antenna structures.

## Acknowledgment

This research was funded by Faculty of Electrical Engineering, Universiti Teknologi MARA and by Holistic Success Module code no. 600-IRMI/DANA 5/3/ARAS (0028/2016).

## References

[1] R. S. A. R. Abdullah, M. F. A. Rasid, M. W. Azis, and M. Khalafalla, "Target prediction in Forward Scattering Radar," *2007 Asia-Pacific Conf. Appl. Electromagn.*, pp. 1–5, Dec. 2007.

[2] M. Cherniakov and R. Abdullah, "Automatic ground target classification using forward scattering radar," *Radar, Sonar Navig. IEE Proc.*, pp. 427–437, 2006.

[3] M. Antoniou, V. Sizov, P. Jancovic, R. Abdullah, N. E. a. Rashid, and M. Cherniakov, "The concept of a forward scattering micro-sensors radar network for situational awareness," *2008 Int. Conf. Radar*, pp. 171–176, Sep. 2008.

[4] V. Sizov, M. Gashinova, N. E. A. Rashid, N. A. Zakaria, and P. Jancovic, "FSR sensors network: performance and parameters," *Proc. Seventh EMRS DTC Tech. Conf.*, no. 1, 2010.

[5] N. E. A. Rashid, M. Antoniou, P. Jancovic, V. Sizov, R. Abdullah, and M. Cherniakov, "Automatic target classification in a low frequency FSR network," *Eur. Radar Conf. (EuRAD 2008)*, pp. 6–9, 2008.

[6] S. A. H. Saghanezhad and Z. Atlasbaf, "Miniaturized Dual-Band CPW-Fed Antennas Loaded with U-Shaped Metamaterials," *IEEE Antennas Wirel. Propag. Lett.*, vol. 14, pp. 658–661, 2015.

[7] D. Mitra, B. Ghosh, A. Sarkhel, and S. R. B. Chaudhuri, "A Miniaturized Ring Slot Antenna Design With Enhanced Radiation Characteristics," *IEEE Trans. Antennas Propag.*, vol. 64, no. 1, pp. 300–305, 2016.

[8] S. Das, P. Chowdhury, A. Biswas, P. P. Sarkar, and S. K. Chowdhury,

"Analysis of a miniaturized multiresonant wideband slotted microstrip antenna with modified ground plane," *IEEE Antennas Wirel. Propag. Lett.*, vol. 14, pp. 60–63, 2015.

[9] B. Kramer, C. Chen, and J. Volakis, "Size reduction of a low-profile spiral antenna using inductive and dielectric loading," *IEEE Antennas Wirel. Propag. Lett.*, vol. 7, pp. 22–25, 2008.

[10] A. Amini, H. Oraizi, and M. A. Chaychi, "Miniaturized UWB Log-Periodic Square Fractal Antenna," *IEEE Antennas Wirel. Propag. Lett.*, vol. 14, pp. 1322–1325, 2015.

[11] Y. F. Weng, S. W. Cheung, and T. I. Yuk, "Design of multiple band-notch using meander lines for compact ultra-wide band antennas," *IET Microwaves, Antennas Propag.*, vol. 6, no. January, p. 908, 2012.

[12] A. K. Gautam, L. Kumar, and B. K. Kanaujia, "Design of Compact F-Shaped Slot Triple-Band Antenna for WLAN / WiMAX Applications," *IEEE Trans. Antennas Propagation,* vol. 64, no. 3, pp. 1101–1105, 2016.

[13] J. Malik, A. Patnaik, and M. V. Kartikeyan, "A Compact Dual-Band Antenna With Omnidirectional Radiation Pattern," *IEEE Antennas Wirel. Propag. Lett.*, vol. 14, pp. 503–506, 2015.

[14] A. Kumar, A. Singh, and E. Sidhu, "Equivalent Circuit Modelling of Microstrip Patch Antenna (MPA) Using Parallel LCR Circuits," *Int. J. Eng. Trends Technol.*, vol. 25, no. 4, pp. 183–185, 2015.

[15] P. Bansal, E. Sidhu, and S. Goyal, "Equivalent Circuit Modeling of Slotted Microstrip Patch Antenna," *Int. J. Res. Eng. Technol.*, pp. 2319–2322, 2014.

[16] S. Jangid and V. S. B. Rama, "An Equivalent Circuit Modeling of UWB Patch Antenna with Band Notched Characteristics," *Eur. J. Adv. Eng. Technol.*, vol. 1, no. 2, pp. 75–79, 2014.

[17] O. O. Olaode, w. D. Palmer, W. T. Joines, and L. Fellow, "Characterization of Meander Dipole Antennas With Lumped Element Model," *IEEE Antennas Wirel. Propag. Lett.*, vol. 11, pp. 346–349, 2012.

[18] M. H. Badjian, C. K. Chakrabarty, S. Devkumar, and G. C. Hock, "Lumped element circuit model approximation of an UWB patch antenna," in *Proceedings - MICC 2009: 2009 IEEE 9th Malaysia International Conference on Communications with a Special Workshop on Digital TV Contents*, 2009, no. December, pp. 28–32.

[19] M. H. Badjian, C. K. Chakrabarty, S. Devkumar, and G. C. Hock, "Circuit modeling of an UWB patch antenna," in *2008 IEEE International RF and Microwave Conference, RFM 2008*, 2008, pp. 3–6.

[20] Z. Sulaiman, A. A., Awang, "Monolithic Microwave Integrated Circuit Filters: Electromagnetic Simulation." p. 61, 2009.